Harmony Search Algorithm based Controller Parameter Optimization for a Distributed Generation System

Mir Nahidul Ambia, Hany M. Hasanien, *Senior Member, IEEE,* Ahmed Al-Durra, *Member, IEEE,* and S. M. Muyeen, *Senior Member, IEEE*

Abstract—This paper presents the utilization of harmony search algorithm (HSA) to optimally design the proportional-integral (PI) controllers of a grid-side voltage source cascaded converter with two additional loops for smooth transition of islanding and resynchronization operations in a distributed generation (DG) system. The first loop is the frequency control loop which is superimposed on the real power set point of the cascaded controller of voltage source converter to minimize the frequency variation during the transition from the grid mode to islanding mode. The second loop is the resynchronization loop which reduces the phase shift of the AC voltages of the DG with the utility grid AC voltages during islanding operation leading to a successful grid reconnection event. The response surface methodology (RSM) is used to build the mathematical model of the system dynamic responses in terms of PI controllers' parameters. The effectiveness of the proposed PI control scheme optimized by the HSA is then compared to that optimization by both genetic algorithm and conventional generalized reduced gradient techniques. The HSA code is built using MATLAB software program. The validity of the proposed system is verified by the simulation results which are performed using PSCAD/EMTDC.

***Index Terms*—Distributed generation, genetic algorithm, grid-side converter, harmony search algorithm, PI controller.**

I. INTRODUCTION

ISLANDING of a grid-connected distributed generation (DG) takes place when the DG is electrically separated from the utility grid. The DG must independently operate successfully with fulfilling the local demand delivered by the DG itself. The traditional power plants are being replaced by the DG system as it is emerging as an alternative substructure in the power systems. Moreover, the increase in DG penetration and presence of multiple DG units has brought the concept of the micro-grid [1], [2]. A micro-grid includes several DG units and local loads and it is connected to the utility grid. The DG units may consist of small modular sources such as wind turbines, fuel cells, photovoltaic systems, and energy storage systems. The renewable energy resources have become popular in AC-DC based hybrid micro-grid systems as the hybrid micro-grid system brings additional benefits for the global system operation and future grid expansion. Among the DG and renewable energy technologies, the growth rate of wind energy has increased enormously in the micro-grid system because of the availability of wind resources and the rapid technical development of the wind farms [3], [4].

During the grid-connected mode, the DG or the micro-grid is connected to the utility grid and during the islanding mode, the utility grid is electrically isolated from the micro-grid leading micro-grid to become the only provider of power to the local loads. Intentional islanding and autonomous operation of the micro-grid system during the islanding modes has drawn a major attraction worldwide [5], [6]. Islanding is an issue to be concerned by the power industries as it might jeopardize the load side equipment if the micro-grid or the DG system cannot operate autonomously. If the micro-grid system fails to operate autonomously during the islanding mode, it might lead to a number of problems for the DG units and local loads including power quality issue and operational problems in the power systems. Due to this reason, the IEEE Std. 1547-2003 states, as one of its tasks for future consideration, the implementation of intentional islanding of the DG systems [7]. The successful islanding and grid reconnection scheme of the micro-grid system can improve the reliability of the system and it also allows utility companies to perform maintenance operations on the utility grid side, if required.

The classical proportional-integral (PI) controllers have been utilized in many control applications due to its robustness and wide stability margin. In this study, the classical PI controllers are used in many places within a hybrid DG system, e.g., with energy storage system, grid-side converter, DC-DC converter of PV sysem, etc. Generally, the cascaded control scheme is used in the AC-DC converter of the DG system as it allows bi-directional real and reactive power control. However, the cascaded control alone is unable to support the islanding operation of induction generator based DG system as the frequency of the system is difficult to be controlled during the transition from grid-connected to islanding mode. To perform the smooth islanding operation, the concept of direct frequency and reactive power control has been introduced into the system with an additional frequency control loop. Moreover, an

Manuscript received January 9th, 2014.

Mir Nahidul Ambia, Ahmed Al-Durra, and S. M. Muyeen are with the Electrical Engineering Department, The Petroleum Institute, Abu Dhabi, U.A.E. (e-mail:aaldurra@pi.ac.ae)

Hany M. Hasanien is with Ain Shams University, Faculty of Engineering, Electrical Power & Machines Department, 11517, Cairo, Egypt.

additional loop has been utilized to perform the resynchronization of the DG system. As the conventional PI controllers are very sensitive to parameter variations and the nonlinearity of the dynamic systems, it is difficult to establish the control sets for islanding and resynchronization tasks. The setting of the PI controller parameters used in a DG system is cumbersome and it is difficult to express this type of DG systems by a mathematical model or transfer function. To achieve the smooth transition between the grid-connected mode to the islanding mode and the islanding mode to the grid reconnected mode, the PI controllers used in the converter should be tuned properly. In our previous studies, the PI controllers in wind energy conversion systems were fine tuned by Taguchi method which is a long statistical method and genetic algorithm (GA) method which is based on the concept of survival of the fittest [8], [9]. Moreover, there is a great development in computational evolutionary optimization techniques which can be used to solve many optimization problems in electric power systems.

The harmony search algorithm (HSA) is one of the newest metaheuristic population search algorithms. It was introduced by Geem *et al*. [10]. The HSA depends mainly on the musical process of searching for a pleasing harmony. The musicians are the decision variables of the function to be optimized. The notes of the musicians represent the decision variable values. The harmony is considered the optimal solution vector. Unlike the gradient optimization techniques, the HSA is a stochastic search and a free derivative algorithm. Furthermore, it has a simple mathematical model and easier in implementation in engineering problems in comparison to other metaheuristic techniques. The HSA has been successfully applied to solve many optimization problems in the power systems [11]-[15].

In this study, the HSA is used to optimally design the PI controllers in cascaded loop of a grid-side voltage source converter including two additional loops for smooth transition of islanding and resynchronization operations of a large DG system. The control scheme consists of four PI controllers of the cascaded control scheme and two extra PI controllers of the two additional loops for islanding and grid resynchronization techniques. The response surface methodology (RSM) is used to build the mathematical model of the dynamic responses of the system in terms of PI controllers' parameters. The parameter optimization of the PI controllers used in hybrid DG systems is a complex task and has so far not been reported in power system literature. Moreover, the proposed technique can be applied to other DG, renewable energy, and power system applications. The effectiveness of the proposed PI control scheme optimized by the HSA is then compared to that optimized by both GA and conventional generalized reduced gradient (GRG) techniques. The HSA code is built using MATLAB software program. The validity of the proposed system is verified by the simulation results which are performed using PSCAD/EMTDC.

II. Model System

Basic architecture of the DG system considered in this study is shown in Fig. 1. The model system consists of a DG unit 1 which has a fixed-speed induction generator-based wind farm and battery energy storage system (BESS) and a DG unit 2 with a photovoltaic (PV) system. Several AC loads and DC loads are connected to the system as distribution network loads. A grid-side converter (GSC), as shown in Fig. 1, with red dotted rectangular box, is connected to the utility grid-side point which performs the islanding and grid resynchronization operation of the DG system.

The data of the induction generators and DG system are illustrated in Tables I and II, respectively. The base MVA of the system is 7.0. This DG system is chosen in this study to present the effectiveness of the proposed optimization technique applied to a complex and non-linear system.

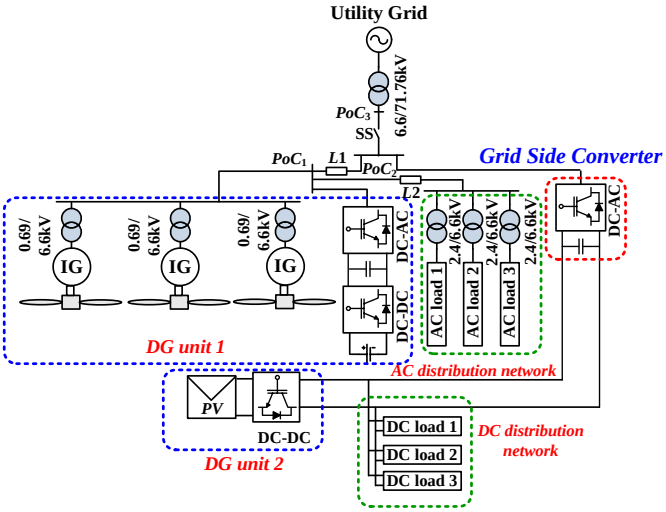

Fig. 1. Basic structure of the DG system.

TABLE I
INDUCTION GENERATOR DATA

Type	Quantity
Rated voltage	0.69 kV
Power	7 MVA
Stator resistance	0.01 pu
Rotor resistance	0.01 pu
Leakage reactance	0.1 pu
Magnetizing reactance	3.5 pu
Rotor mutual reactance	0.12 pu
Inertia constant	3 s

TABLE II
DG SYSTEM DATA

Parameters	Quantity
Base MVA	7 MVA
Rated voltage	6.6 kV
DC generation	0.5 MW
AC load	2.21 MW, 2.4 kV
DC load	2.13 MW, 6.6 kV
DC bus voltage	6.6 kV
DC link capacitance	100000 µF
Converter Set point (P_{conv}^{*})	-1.63MW
PoC_2 voltage set point (V_{PoC2}^{*})	1.0 pu
Line impedance (L_1)	0.01+j0.035 pu
Line impedance (L_2)	0.001+j0.002 pu

III. Wind Turbine Model

The wind turbine extracted power (P_W) can be expressed as follows [16]:

$$P_W = \tfrac{1}{2}\rho\pi R^2 C_p(\lambda,\beta) {V_w}^3 \quad (1)$$

where ρ is the air density, R is the radius of the turbine, V_w is the wind speed, $C_P(\lambda,\beta)$ is the power coefficient given by (2), where the tip speed ratio λ is given by (3) in terms of the turbine rotational speed ω.

$$C_p(\lambda.\beta) = \tfrac{1}{2}(\lambda - 0.022\beta^2 - 5.6)e^{-0.17\lambda} \quad (2)$$

$$\lambda = \frac{\omega R}{V_w} \quad (3)$$

The wind turbine and the wind generator are modeled as a one mass lumped model with a constant inertia [17]. The step up gearbox is assumed to be lossless and is represented by a simple gain [18]. Aggregated wind farm model where several wind generators are expressed by a large wind generator is considered in this study to speed up the simulation of the complex DG system.

IV. PV Model

The PV systems convert solar radiation into electrical energy. A practical PV system can be modeled by a current source in parallel with a diode and a combination of a series resistance and a parallel resistance [19]. The current source represents the photo current, which is a function of incident solar radiation and temperature. The diode represents the reverse saturation current due to the p-n junction of the solar cell while the resistances account for the losses [19].

V. Control Strategy of GSC

When the DG is disconnected from the utility grid, the power balance is lost in the system which leads the DG system to a variation of AC voltage magnitude and frequency. This results in the DG system to become unstable. Usual practice of using the power converter connected to the grid-side point (PoC_2) as shown in Fig. 1 is to control the real and reactive powers between AC and DC sides. The conventional cascaded control strategy is shown in the blue dotted rectangular box of Fig. 2. The real and reactive powers are controlled according to the set points in the control strategy. The d-axis current controls the real power and q-axis current maintains the terminal voltage at the PoC_2. The transformation angle (θ_{PLL}) is obtained from the phase locked loop (PLL) which uses the grid-side three-phase voltages at the input of the PLL system.

An additional loop of direct frequency control is introduced to the real power control loop as shown with brown dotted rectangular box helping the DG system to minimize the variation of the frequency during the islanding event. Instead of using another converter, the additional power transfer required (ΔP_f) in this loop is superimposed on the active power set point which in turn maintains the frequency of the system during transition from the grid-connected mode to the islanding mode. The direct frequency control loop is enabled during the islanding event with a latch system.

Another important issue in the islanding events is the grid resynchronization technique. For a successful grid reconnection mode, it is important to resynchronize the voltages of the DG with voltages of the utility grid. During the islanding event, the DG AC voltage is phase shifted from the utility grid voltages despite of the voltage magnitude and frequency regulation. In order to have a soft transition from the islanding mode to grid reconnection mode, an additional loop with green dotted block is added to the real power of the cascaded control as shown in Fig. 2. The voltage signals of DG (PoC_2) and utility grid (PoC_3) as shown in Fig. 1 are taken in α-β frame for the resynchronization block in Fig. 2. This algorithm is used to track the phase difference between the utility grid voltages and DG AC voltages. The PI controller used in the loop uses the error signal to synchronize them. The voltages are taken in α-β frame because the transformation angle for d-q frame is unknown during islanding mode as the utility grid is disconnected from the system. The additional power (ΔP_{sync}) is introduced to adjust the AC voltage phase for synchronizing it with utility grid voltages before reconnection point. This additional loop is enabled 2 s prior to the grid reconnection point.

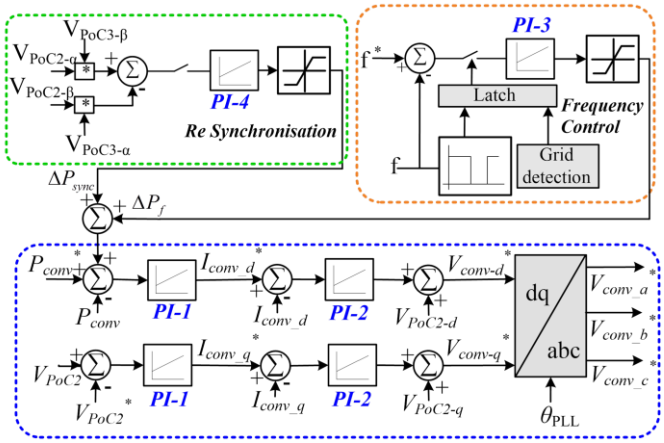

Fig. 2. Direct frequency and reactive power islanding control of GSC

In this control strategy, six PI controllers are used for successful islanding and grid resynchronization strategy. However, the number of PI controllers of the outer loop and inner loop of real and reactive power control is minimized into two considering them as identical which reduces the total PI controllers from six to four. An optimal design procedure of parameters of four PI controllers are given in the following section as manual tuning of these PI controllers for islanding and grid-resynchronization operations is cumbersome and time consuming. Therefore, this study attempts to optimally design the parameters with eight design variables. The optimization approach is done using the HSA.

VI. Optimal Design

A. The RSM

The RSM is a statistical method used to build a mathematical model by obtaining the relationship between the design variables and the response [20]. In this study, PSCAD/EMTDC [21] is used for numerical simulations to provide the response. The frequency deviation factor (FDF) after islanding (y_1), the settling time of the frequency response after islanding (y_2), the

maximum percentage overshoot (MPOS) of the frequency response after grid reconnection (y_3), the settling time of the frequency response after grid reconnection (y_4), and the frequency deviation factor after grid reconnection (y_5) are the responses. These are varied by the design variables variant. In the RSM, the second order model is used to obtain an accurate response.

B. The HSA

The brief explanation of the HSA can be represented by five steps as follows:

Step 1: Initialize the problem and algorithm parameters

In this step, the optimization problem can be specified as follows:

$$\text{Minimize } f(x) \text{ subject to } x_i \in X_i,\ i = 1, 2, \ldots N \quad (4)$$

where *f(x)* is an objective function, *x* is a set of the decision variables x_i, *N* is the number of decision variables, and X_i is the range of each decision variable. The parameters of the HSA to be initialized are the harmony memory size (HMS) which illustrates the number of solution vectors in the harmony memory, harmony memory considering rate (HMCR), pitch adjusting rate (PAR), and the number of improvisations (NI) or stopping criteria.

Step 2: Initialize the harmony memory (HM)

The HM matrix is initialized with many randomly generated vectors up to the HMS.

$$HM = \begin{bmatrix} x_1^1 & x_2^1 & \ldots\ldots x_{N-1}^1 & x_N^1 \\ x_1^2 & x_2^2 & \ldots\ldots x_{N-1}^2 & x_N^2 \\ \vdots & \vdots & \vdots & \vdots \\ x_1^{HMS} & x_2^{HMS} & \ldots\ldots x_{N-1}^{HMS} & x_N^{HMS} \end{bmatrix} \quad (5)$$

Step 3: Improvise a new harmony

A new harmony vector $x^n = (x_1^n, x_2^n, \ldots, x_N^n)$ is produced based on the HMCR, PAR, and random selection. The HMCR is the choice rate of one value from the historical values stored in the HM while (1-HMCR) is the selecting rate randomly of one value from the possible range. x_i^n can be written as follows:

$$x_i^n \leftarrow \begin{cases} x_i^n \in \{x_i^1, x_i^2, \ldots, x_i^{HMS}\} \quad with \quad probability \quad HMCR \\ x_i^n \in X_i \quad with \quad probability \quad (1 - HMCR) \end{cases} \quad (6)$$

For example, the HMCR of 0.8 illustrates that the HSA will choose the decision variable from the stored values in the HM with 80 % probability and from the entire possible range with 20 %. All the components selected by the harmony consideration are checked by pitch adjusting decision as follows:

$$x_i^n \leftarrow \begin{cases} Yes \quad with \quad probability \quad PAR \\ No \quad with \quad probability \quad (1 - PAR) \end{cases} \quad (7)$$

The decision No means nothing to do and the decision Yes makes x_i^n to be modified as follows:

$$x_i^n = x_i^n \pm rand() * bw \quad (8)$$

where bw is an arbitrary distance bandwidth and rand( ) is a random number varying from 0 to 1. The PAR can be adjusted by the following equation:

$$PAR(g) = PAR_{\min} + \frac{(PAR_{\max} - PAR_{\min})}{NI} * g \quad (9)$$

where g = 1, 2, …,NI, PAR(g) is the PAR for improvisation of g, PAR_{min} is the minimum PAR, and PAR_{max} is the maximum PAR.

Step 4: Update the HM

In this step, the HM is updated based on the fitness function value. If the new harmony vector x^n has a better fitness function than the worst harmony in the HM, x^n will replace it in the HM.

Step 5: Check termination criteria

If NI is reached, the HSA will stop, otherwise the steps three and four will repeat [12].

VII. Optimization Procedure

The proportional gain and integral time constant of the PI controllers shown in Fig. 2 are the design variables. X_1, X_3, X_5, and X_7 are the proportional gain of PI-1, PI-2, PI-3, and PI-4, respectively. X_2, X_4, X_6, and X_8 are their integral time constants. These design variables have three levels. The levels (-1), (0), and (1) represent the minimum, average, and maximum values of the design variable, respectively. The RSM model is based on the central composite design in building the responses. There are 90 design experiments for eight design variables problem, as shown in Table A1 in Appendix. This statistical design is performed using Minitab program [22]. The PSCAD program calculation is carried out for each experiment and the values of y_1 to y_5 are stored in Table A1. The fitted RSM model is shown in details in Appendix. The HSA is applied to the RSM model. The HSA code is built using MATLAB program [23]. y_3 is the objective function and the other functions are nonlinear constraint functions. The design variable range and constraints of the optimization problem are described as follows:

- Design variables range is $2.0 \le X_1 \le 3.5$, $0.004 \le X_2 \le 0.01$, $1.0 \le X_3 \le 3$, $0.01 \le X_4 \le 0.02$, $10 \le X_5 \le 18$, $0.01 \le X_6 \le 0.02$, $0.01 \le X_7 \le 0.08$, and $1.0 \le X_8 \le 6$
- The constraints are $y_1 \le 1.8$ %, $y_2 \le 0.5$ s, $y_4 \le 1$ s, and $y_5 \le 0.2$ %.

The parameters of the HSA are shown in Table III. Fig. 3 shows the fitness function convergence. Table IV shows the optimization set value and level of the design variables using the HSA method. At these optimal values, y_3 is 0.35 %.

For a fair comparison, GA and GRG techniques are also applied to the RSM model. In GA analysis, the Rank fitness scaling is applied to avoid premature convergence. GA includes natural selection, mutation, and crossover. The selection process is performed using the uniform selection technique which prevents bias and minimal spread. The GA characteristics are illustrated in Table V. Fig. 4 shows the fitness function convergence and current best individual. In the GRG technique, the derivatives are approximated by the solver

in the objective function. The number of iterations is 1000. The objective function tolerance is $1.0e^{-6}$. The optimal level and size value of the design variables using GA and GRG techniques are also shown in Table IV.

TABLE III
PARAMETERS OF THE HSA

HMS	30
HMCR	0.9
PAR_{min}	0.4
PAR_{max}	0.9
NI	1000

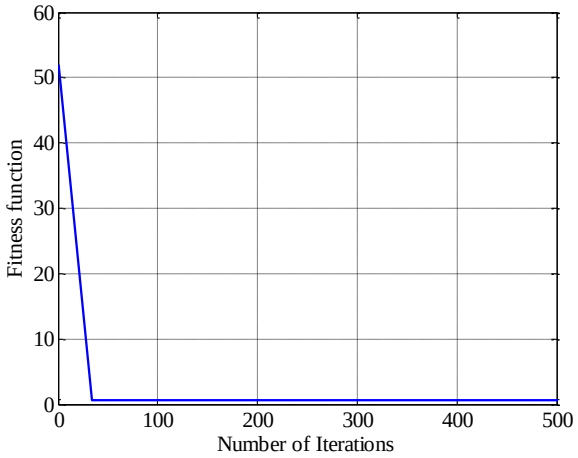

Fig. 3. Fitness function convergence using the HSA.

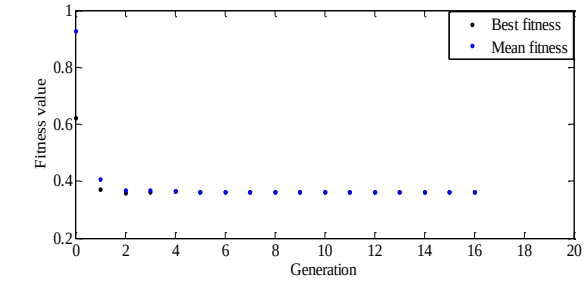

(a)

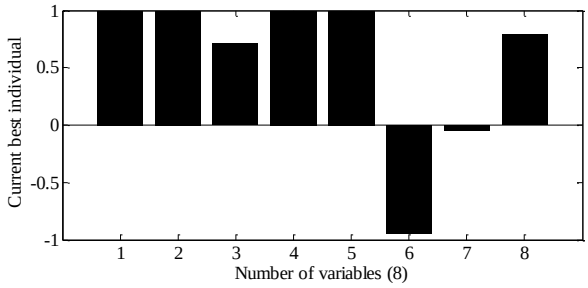

(b)

Fig. 4. GA results (a) Fitness function convergence. (b) Current best individual.

VIII. SIMULATION ANALYSIS AND DISCUSSION

The effectiveness of the proposed HSA based controller parameters optimization technique in islanding and grid resynchronization of the DG system is demonstrated in this section. In the DG system wind generator connected at AC bus is generating variable power as per wind availability. BESS connected at PoC1 is smoothing the fluctuating power and delivering towards line L_1 shown in Fig. 1. In the grid-connected mode, immediate before the islanding operation takes place, the power at Line L_1 was around 4.3 MW (shown in Fig. 5), DG was delivering 0.5 MW to the main grid and after fedding to the AC load and considering power loss in the line remaining 1.45 MW was transmitting to the dc bus through converter. At 5 s, the utility grid is disconnected to initiate the islanding operation. The islanding operation continues for 20 s. At 25 s, the grid is reconnected to the micro-grid, 2 s prior to the grid-reconnection mode, at 23 s the resynchronization is enabled by the resynchronization controller.

Figures 5 to 11 show the islanding operation of the hybrid DG system using the direct frequency and reactive power control method when the cage induction generator based wind turbine is driven by real wind speed. Fig. 5 shows the wind farm fluctuating output power (green color) and smoothen power at the line side. Figs. 6 to 8 reflect the induction generator frequency, wind farm terminal voltage and converter terminal voltage at PoC2 accordingly. Due to the additional frequency control loop shown in Fig. 2, the frequency of induction generator shown in Fig. 6 remains constant at pre-islanding state and after islanding occurs at 5 s. The oscillation in frequency response shown in Fig. 6 at 23 s is due to the activation of resynchronization loop in Fig. 2. Figs. 7 and 8 show that HSA is an effective tool to tune the PI controlelrs shown in Fig. 2 that leads to successful islanding and reconnection of the DG system. Figs. 7 and 8 also show that HSA is superior to GA and GRG methods in terms of quick voltage recovery and less oscillations. Fig. 9 shows the power from the utility grid where only zoom view of response from 24 to 30 s is demonstrated. It can be seen from this figure that before 25 s, during islanding mode, the grid power is zero. After grid reconnection mode, the utility grid starts injecting power into the micro-grid. Figures 10 and 11 show the converter power from ac to dc bus and AC load consumption accordingly. It is also seen from Fig. 9 that HSA is a better optimization tool compared to GA and GRG that works well with this complex nonlinear system.

TABLE IV
OPTIMAL LEVEL AND SIZE OF DESIGN VARIABLES

Level & Size	X_1	X_2	X_3	X_4	X_5	X_6	X_7	X_8
Level (HSA)	-0.10	-0.96	0.96	-0.01	0.92	0.03	0.16	-0.35
Size (HSA)	2.67	0.004	2.96	0.014	17.68	0.015	0.05	2.62
Level (GA)	0.99	1.0	0.71	1	1	-0.94	-0.05	0.78
Size (GA)	3.49	0.01	2.71	0.02	18	0.01	0.043	5.45
Level (GRG)	-1	-1	1	1	1	-1	-0.06	1
Size (GRG)	2	0.004	3	0.02	18	0.01	0.043	6

TABLE V
GA CHARACTERISTICS

Population type	Double vector
Population size	50
Fitness scaling function	Rank
Selection function	Uniform
Crossover fraction	0.8
Crossover function	Scattered
Migration fraction	0.2
Migration interval	20

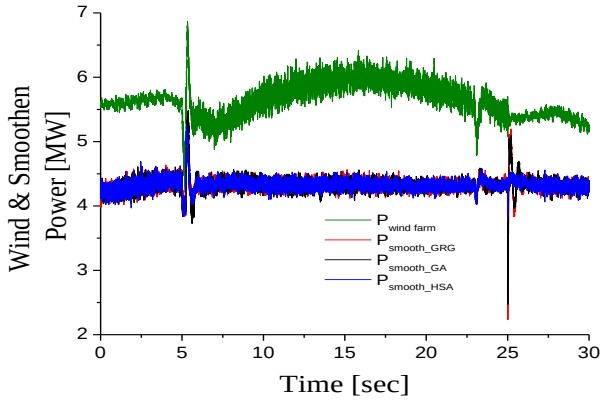

Fig. 5. Real power of wind farm along with line power.

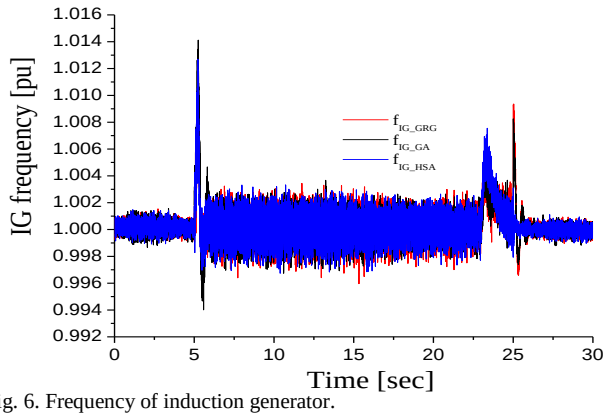

Fig. 6. Frequency of induction generator.

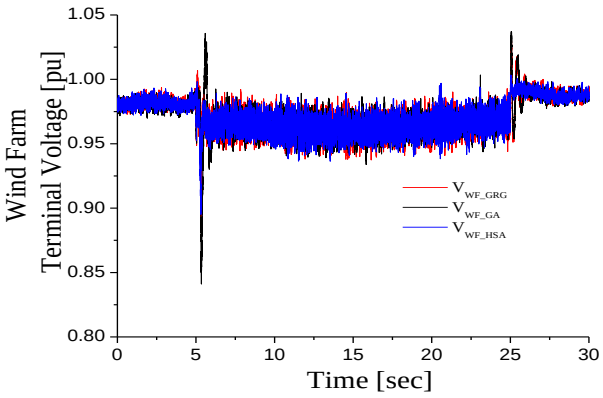

Fig. 7. Terminal voltage at wind farm.

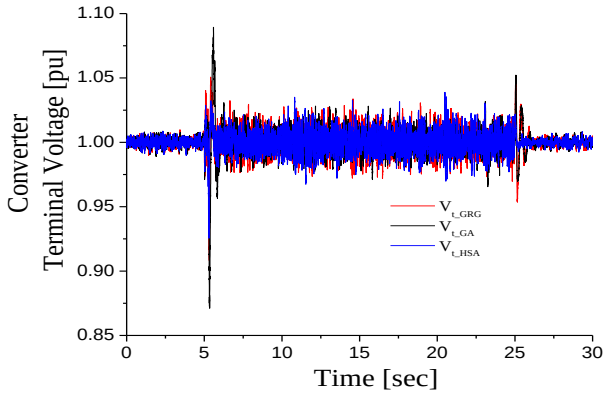

Fig. 8. Terminal voltage at converter side (PoC2).

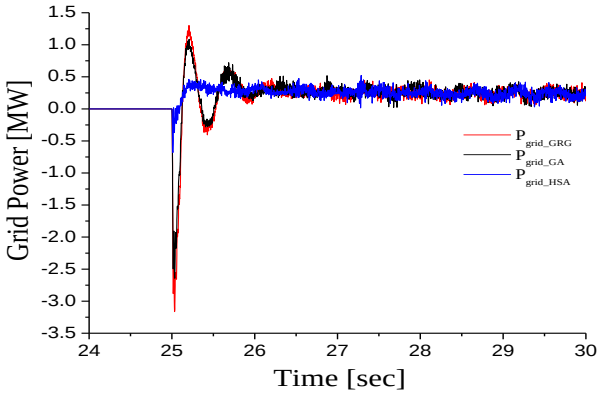

Fig. 9. Real power at the grid.

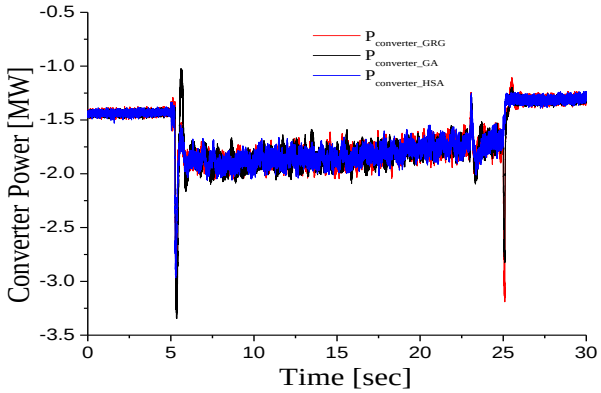

Fig. 10. Real power through converter.

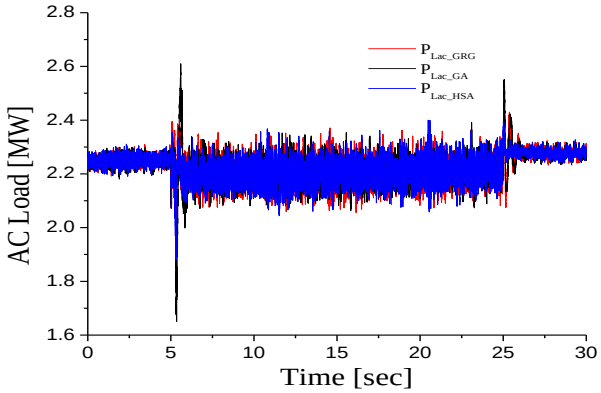

Fig. 11. Real power at AC load.

IX. Conclusion

In this paper, a step by step optimum design procedure of multiple PI controllers' parameters is demonstrated using Harmony Search Algorithm and Response Surface Method based schemes. The parameter optimization scheme is applied for islanding and grid resynchronization of distributed generation system where multiple PI controllers are used in cascaded control loops to control real and reactive power simultaneously along with two additional loops for smooth transition of islanding and resynchronization operations. The effectiveness of the proposed HSA methodology in obtaining optimum PI controller parameters in a complex and nonlinear system is demonstrated by comparing the results using two other popular techniques namely Genetic Algorithm and

Generalized Reduced Gradient methods. It is found that HSA is an effective method to optimally determine the parameters of multiple PI controllers in cascaded control of power converter used in the Distributed Generation system for successful islanding and grid-resynchronizing operations. The proposed technique is equally applicable to different renewable energy, energy storage system, and power system applications when the nonlinear system is difficult to express with mathematical model.

APPENDIX

TABLE A1

RANGE OF DESIGN VARIABLES AND EXPERIMENT FREQUENCY

Exp.	X_1	X_2	X_3	X_4	X_5	X_6	X_7	X_8	y1 (%)	y2 (s)	y3 (%)	y4 (s)	y5 (%)
1	0	0	0	0	-1	0	0	0	1.89	0.63	0.833	0.59	0.197
2	0	0	0	0	0	0	0	0	1.86	0.59	0.813	0.99	0.33
3	0	0	0	0	0	0	0	0	1.86	0.59	0.813	0.99	0.33
4	1	-1	1	1	1	-1	-1	1	1.73	0.31	0.57	1.36	1.3
5	-1	1	1	1	1	-1	-1	1	1.97	0.85	0.68	1.8	1.71
6	-1	1	-1	1	-1	-1	1	-1	1.8	0.78	1.18	1.6	0.84
7	-1	1	1	1	-1	-1	-1	-1	2.21	1.24	0.85	1.47	0.51
8	1	1	1	-1	1	1	-1	1	1.69	0.6	0.7	1.36	0.3
9	1	1	1	1	1	-1	1	-1	1.91	0.61	0.7	0.85	0.59
10	1	1	1	1	-1	-1	1	1	2.03	1.22	0.77	1.42	1.4
11	1	-1	-1	-1	-1	-1	-1	-1	1.74	0.52	1.1	1.58	0.7
12	-1	-1	1	-1	1	1	-1	1	1.68	0.38	0.68	1.15	0.43
13	-1	1	-1	-1	1	1	-1	-1	1.93	0.62	1.05	1.27	0.3
14	1	1	1	1	1	1	1	1	1.8	0.68	0.7	1.22	0.4
15	1	-1	-1	-1	1	-1	-1	1	1.75	0.48	1	2	2.89
16	-1	1	-1	-1	-1	1	-1	1	2	0.98	0.82	1.37	0.31
17	1	-1	-1	-1	-1	1	-1	1	1.73	0.6	1.31	1.47	0.3
18	-1	1	-1	1	1	-1	1	1	1.86	0.79	0.9	1.72	1.85
19	0	0	0	0	0	0	0	1	1.81	0.59	0.74	1.11	0.37
20	-1	-1	-1	1	-1	-1	-1	1	1.76	0.78	0.73	1.84	1.65
21	1	1	-1	1	1	1	-1	1	1.73	0.51	0.92	1.55	0.248
22	0	0	0	1	0	0	0	0	1.68	0.29	0.75	1.35	0.2
23	-1	1	1	-1	-1	1	1	1	2	1.11	0.8	0.58	0.35
24	-1	-1	-1	-1	-1	1	1	-1	1.95	0.5	1.27	0.78	0.26
25	0	1	0	0	0	0	0	0	1.8	0.61	0.81	1.31	0.26
26	1	1	-1	-1	-1	1	1	-1	1.9	1.02	1.5	1.38	0.27
27	0	-1	0	0	0	0	0	0	1.63	0.3	0.73	1.17	0.4
28	1	-1	1	-1	1	1	1	-1	1.8	0.38	0.89	0.88	0.24
29	-1	0	0	0	0	0	0	0	1.92	0.57	0.73	1.22	0.45
30	1	-1	1	-1	-1	-1	1	-1	2.05	0.64	0.79	0.99	0.68
31	-1	-1	-1	-1	1	-1	1	-1	1.94	0.49	1.2	1.89	0.85
32	1	1	-1	-1	-1	-1	1	1	2	0.93	1.19	1.9	2.13
33	0	0	0	0	0	0	0	0	1.86	0.59	0.813	0.99	0.33
34	1	1	-1	1	1	-1	-1	-1	1.94	0.85	1.01	1.9	0.94
35	0	0	0	0	0	1	0	0	1.83	0.32	0.86	0.88	0.39
36	1	1	-1	-1	1	1	1	1	1.79	0.64	1.19	1.76	0.47
37	0	0	0	0	0	0	0	0	1.86	0.59	0.813	0.99	0.33
38	1	-1	-1	1	1	1	1	-1	1.9	0.39	1.32	1.87	0.62
39	1	-1	1	-1	1	-1	1	1	1.8	0.55	0.78	1.28	1.37
40	0	0	0	-1	0	0	0	0	1.65	0.49	0.86	1.16	0.26
41	-1	-1	-1	1	1	1	-1	1	1.61	0.3	0.86	1.7	0.28
42	1	1	1	1	-1	1	1	-1	1.91	1.01	1.06	1.08	0.28
43	-1	1	1	-1	-1	-1	1	-1	2.43	2.72	0.86	1.46	0.65
44	1	-1	1	1	1	1	-1	-1	1.64	0.32	0.85	0.99	0.269
45	-1	1	1	-1	1	-1	1	1	2.29	0.88	0.64	0.87	1.2
46	-1	1	1	-1	1	1	1	-1	1.91	0.62	0.84	0.88	0.25
47	0	0	0	0	0	0	1	0	1.77	0.59	0.88	1.17	0.51
48	1	1	1	-1	1	-1	-1	-1	1.87	0.65	0.83	1.54	0.59
49	0	0	0	0	0	0	0	0	1.86	0.59	0.813	0.99	0.33
50	0	0	-1	0	0	0	0	0	1.93	0.57	1	1.61	0.56
51	-1	1	1	1	-1	1	-1	1	2	0.99	0.81	1.35	0.4
52	1	-1	-1	1	-1	1	1	1	1.94	1	2.67	1.97	0.57
53	-1	-1	1	1	-1	-1	1	1	1.76	0.61	0.72	1.11	1.37
54	0	0	0	0	0	0	0	0	1.86	0.59	0.813	0.99	0.33
55	1	-1	-1	-1	1	1	-1	-1	1.61	0.32	1.23	1.59	0.47
56	0	0	0	0	0	-1	0	0	2.03	0.59	0.65	1.16	0.94
57	1	1	-1	1	-1	-1	-1	1	2.05	0.88	0.91	1.98	1.86
58	-1	-1	-1	-1	1	1	1	1	1.82	0.3	1.09	1.98	0.44
59	0	0	0	0	0	0	0	0	1.86	0.59	0.813	0.99	0.33
60	1	1	-1	-1	1	-1	1	-1	1.89	0.57	1.27	1.9	1.1
61	-1	-1	-1	1	1	-1	-1	-1	1.69	0.47	0.83	1.7	0.72
62	1	-1	-1	1	-1	-1	1	-1	2.13	0.61	1.39	1.98	1.29
63	0	0	0	0	1	0	0	0	1.8	0.32	0.75	0.94	0.31
64	1	-1	1	1	-1	-1	-1	-1	2.03	0.65	0.77	1.13	0.43
65	0	0	0	0	0	0	-1	0	1.93	0.59	1.16	0.76	0.08
66	0	0	1	0	0	0	0	0	2.02	0.69	0.63	1.01	0.37
67	-1	-1	-1	-1	-1	-1	1	1	2.05	0.57	0.91	1.9	1.75
68	1	-1	1	1	-1	1	-1	1	1.778	0.35	0.7	1.17	0.21
69	1	1	1	-1	-1	-1	-1	1	2.02	1.56	0.69	1.51	1.34
70	-1	1	1	1	1	1	-1	-1	1.96	0.68	0.8	0.97	0.4
71	-1	1	-1	-1	-1	-1	-1	-1	2.24	2.03	1.06	1.65	0.61
72	-1	1	-1	1	-1	1	1	1	1.87	0.63	1.16	1.94	0.59
73	0	0	0	0	0	0	0	0	1.86	0.59	0.813	0.99	0.33
74	-1	-1	1	1	-1	1	1	-1	1.72	0.4	0.98	0.63	0.29
75	-1	-1	1	-1	1	-1	-1	-1	1.87	0.6	0.63	1.19	0.32
76	-1	-1	1	1	1	-1	1	-1	1.84	0.34	0.66	1.23	0.52
77	0	0	0	0	0	0	0	-1	1.92	0.48	0.88	0.74	0.18
78	-1	-1	1	-1	-1	-1	-1	1	1.88	0.58	0.67	0.95	1.28
79	1	-1	-1	1	1	-1	1	1	1.9	0.32	0.91	1.98	2.7
80	1	0	0	0	0	0	0	0	1.91	0.57	0.73	1.22	0.46
81	1	1	1	-1	-1	1	-1	-1	1.97	0.7	1.05	0.76	0.39
82	1	1	-1	1	-1	1	-1	-1	1.83	0.62	1.39	1.15	0.2
83	-1	1	-1	1	1	1	1	-1	2.07	0.6	1.22	1.26	0.08
84	-1	-1	1	1	1	1	1	1	1.62	0.35	0.73	1.03	0.3
85	1	-1	1	-1	-1	1	1	1	1.95	0.65	0.79	1.31	0.36
86	0	0	0	0	0	0	0	0	1.86	0.59	0.813	0.99	0.33
87	-1	-1	1	-1	-1	1	-1	-1	1.87	0.78	0.9	0.74	0.41
88	0	0	0	0	0	0	0	0	1.86	0.59	0.813	0.99	0.33
89	-1	1	-1	-1	1	-1	1	1	2.01	0.85	0.68	1.89	1.68
90	-1	-1	-1	1	-1	1	-1	-1	1.71	0.36	1.18	0.99	0.23

Equatioins-Objective function and Contrants:

$$Y_1 = 1.84802 - 0.0230606x_1 + 0.0727576x_2 + 0.0142121x_3 - 0.0257879x_4 - 0.0542121x_5 - 0.0598788x_6 + 0.0298788x_7 - 0.0227576x_8 + 0.0755426x_1^2 - 0.124457x_2^2 + 0.135543x_3^2 - 0.174457x_4^2 + 0.00554259x_5^2 + 0.0905426x_6^2 + 0.0105426x_7^2 - 0.0227576x_8^2 - 0.0457500x_1x_2 - 0.00862500x_1x_3 + 0.0485625x_1x_4 - 0.0176250x_1x_5 + 0.000125000x_1x_6 + 0.0164375x_1x_7 + 0.00825000x_1x_8 + 0.0198750x_2x_3 - 0.00418750x_2x_4 + 0.00325000x_2x_5 - 0.00887500x_2x_6 - 0.0320625x_2x_7 + 0.00112500x_2x_8 - 0.00956250x_3x_4 - 0.0151250x_3x_5 - 0.0161250x_3x_6 - 0.0129375x_3x_7 - 0.00925000x_3x_8 + 0.0120625x_4x_5 + 0.0110625x_4x_6 - 0.0201250x_4x_7 - 0.00581250x_4x_8 + 0.00550000x_5x_6 + 0.0123125x_5x_7 - 7.50000E-04x_5x_8 + 0.00456250x_6x_7 + 0.000750000x_6x_8 + 0.000812500x_7x_8$$

$$Y_2 = 0.532047 - 0.046061x_1 + 0.209545x_2 + 0.042727x_3 - 0.068485x_4 - 0.167121x_5 - 0.103182x_6 + 0.007576x_7 - 0.011364x_8 + 0.079348x_1^2 - 0.035652x_2^2 + 0.139348x_3^2 - 0.100652x_4^2 + -0.015652x_5^2 - 0.035652x_6^2 + 0.099348x_7^2 + 0.044348x_8^2 - 0.056250x_1x_2 - 0.022812x_1x_3 + 0.052500x_1x_4 + 0.018125x_1x_5 + 0.053438x_1x_6 + 0.032812x_1x_7 + 0.057812x_1x_8 + 0.045938x_2x_3 - 0.043125x_2x_4 - 0.064375x_2x_5 - 0.066563x_2x_6 - 0.001562x_2x_7 - 0.024687x_2x_8 - 0.019687x_3x_4 - 0.032812x_3x_5 - 0.023125x_3x_6 + 0.04x_3x_7 - 0.0075x_3x_8 + 0.05x_4x_5 + 0.035938x_4x_6 - 0.002187x_4x_7 + 0.033438x_4x_8 + 0.042188x_5x_6 - 0.016562x_5x_7 + 0.022188x_5x_8 + 0.028750x_6x_7 + 0.036875x_6x_8 - 0.000625x_7x_8$$

$$Y_3 = 0.800992 - 0.069091x_1 - 0.012121x_2 - 0.180758x_3 + 0.006212x_4 - 0.071258x_5 + 0.087727x_6 + 0.068788x_7 - 0.062424x_8 - 0.062415x_1^2 - 0.022415x_2^2 + 0.022585x_3^2 + 0.012585x_4^2 - 0.000915x_5^2 - 0.037415x_6^2 + 0.227585x_7^2 + 0.017585x_8^2 - 0.023437x_1x_2 - 0.059062x_1x_3 + 0.002188x_1x_4 - 0.028125x_1x_5 + 0.025000x_1x_6 + 0.015000x_1x_7 + 0.020000x_1x_8 + 0.034688x_2x_3 - 0.011562x_2x_4 + 0.010625x_2x_5 - 0.031250x_2x_6 - 0.021250x_2x_7 - 0.035000x_2x_8 - 0.014063x_3x_4 + 0.024375x_3x_5 - 0.035000x_3x_6 - 0.058750x_3x_7 - 0.001250x_3x_8 - 0.040625x_4x_5 + 0.030625x_4x_6 + 0.025000x_4x_7 + 0.016875x_4x_8 - 0.031562x_5x_6 - 0.021562x_5x_7 - 0.009688x_5x_8 + 0.017187x_6x_7 + 0.012188x_6x_8 + 0.025312x_7x_8$$

$$Y_4 = 1.01893 + 0.05939x_1 + 0.01697x_2 - 0.26939x_3 + 0.03591x_4 + 0.05712x_5 - 0.14727x_6 - 0.00045x_7 + 0.11379x_8 + 0.18041x_1^2 + 0.20041x_2^2 + 0.27041x_3^2 + 0.21541x_4^2 - 0.27459x_5^2 - 0.01959x_6^2 - 0.07459x_7^2 - 0.11459x_8^2 - 0.02437x_1x_2 - 0.01625x_1x_3 - 0.02188x_1x_4 - 0.01437x_1x_5 + 0.02906x_1x_6 + 0.02969x_1x_7 + 0.00312x_1x_8 + 0.04656x_2x_3 + 0.00281x_2x_4 - 0.04906x_2x_5 - 0.02687x_2x_6 - 0.04625x_2x_7 - 0.01469x_2x_8 + 0.00844x_3x_4 - 0.02406x_3x_5 + 0.02063x_3x_6 - 0.07500x_3x_7 - 0.02781x_3x_8 - 0.04344x_4x_5 + 0.01625x_4x_6 + 0.00187x_4x_7 + 0.02406x_4x_8 + 0.03375x_5x_6 - 0.03562x_5x_7 - 0.02594x_5x_8 + 0.03719x_6x_7 + 0.06625x_6x_8 - 0.00813x_7x_8$$

$$Y_5 = 0.320685 + 0.061924x_1 - 0.021227x_2 - 0.134076x_3 + 0.004500x_4 + 0.030758x_5 - 0.431106x_6 + 0.042621x_7 + 0.262561x_8 + 0.140968x_1^2 + 0.015968x_2^2 + 0.150968x_3^2 - 0.084032x_4^2 - 0.060532x_5^2 + 0.350968x_6^2 - 0.019032x_7^2 - 0.039032x_8^2 - 0.039391x_1x_2 - 0.071234x_1x_3 - 0.014734x_1x_4 + 0.035266x_1x_5 - 0.055047x_1x_6 + 0.026297x_1x_7 + 0.006859x_1x_8 + 0.050359x_2x_3 + 0.005609x_2x_4 - 0.030641x_2x_5 + 0.005922x_2x_6 - 0.016547x_2x_7 - 0.010359x_2x_8 + 0.001266x_3x_4 - 0.034984x_3x_5 + 0.124078x_3x_6 - 0.038453x_3x_7 - 0.052141x_3x_8 - 0.004734x_4x_5 - 0.011297x_4x_6 + 0.035672x_4x_7 + 0.001859x_4x_8 - 0.027547x_5x_6 - 0.033078x_5x_7 + 0.023109x_5x_8 - 0.017766x_6x_7 - 0.236578x_6x_8 - 0.004047x_7x_8$$

REFERENCES

[1] Aa N. D. Hatziargyriou and A. P. S. Meliopoulos, "Distributed energy sources: Technical challenges," in *Proc. IEEE Power Eng. Soc. Winter Meeting*, vol. 2, New York, 2002, pp. 1017–1022.

[2] C. L. Smallwood, "Distributed generation in autonomous and nonautonomous micro grids," *in Proc. Rural Electric Power Conf.*, 2002, pp. D1–D1-6.

[3] The Global Wind Energy Council, Global Wind Report, Annual market update 2010. Available: http://www.gwec.net/

[4] N. K. Ardeshna and B. H. Chowdhury, "Optimizing Micro-grid Operations in the Presence of Wind Generation," *Power Symposium*, NAPS'08, 28-30 Sept. 2008.

[5] H. You, V. Vittal, and Z. Yang, "Self-healing in power systems: An approach using islanding and rate of frequency decline-based load shedding," *IEEE Trans. Power Syst.*, vol. 18, no. 1, pp. 174-181, Feb. 2002.

[6] R. Fulton and C. Abbey, "Planned islanding of 8.6 MVA IPP of BC Hydro system reliability," in *Proc. 2004 First Int. Conf. Integr. RE DER*, pp. 1-9.

[7] IEEE Standard for Interconnecting Distributed Resources With Electric Power Systems, IEEE Std 1547-2003, pp. 01-16, 2003.

[8] Hany M. Hasanien, and S. M. Muyeen, "A Taguchi approach for optimum design of proportional-integral controllers in cascaded control scheme", *IEEE Transactions on Power Systems*, vol. 28, no. 2, pp. 1636–1644, May 2013.

[9] Hany M. Hasanien, and S. M. Muyeen, "Design optimization of controller parameters used in variable speed wind energy conversion system by genetic algorithms", *IEEE Transactions on Sustainable Energy*, vol. 3, no. 2, pp. 200-208, April 2012.

[10] Geem Z.W., Kim J.H., and Loganathan G.V., "A new heuristic optimization algorithm: harmony search", *Simulation*, vol. 76, no. 2, pp. 60-68, 2001.

[11] Rayapudi S.R., Sadhu V.L.N., Manyala R.R., and A. Srinivasa R., "Optimal network reconfiguration of large-scale distribution system using harmony search algorithm", *IEEE Transactions on Power Systems*, vol. 26, no. 3, pp. 1080–1088, August 2011.

[12] A. Verma, B.K. Panigrahi, and P.R. Bijwe, "Harmony search algorithm for transmission network expansion planning", *IET Generation, Transmission and Distribution*, vol. 4, no. 6, pp. 663–673, 2010.

[13] L. Wei, W. Guo, F. Wen, G. Ledwich, Z. Liao, and J. Xin, "Waveform matching approach for fault diagnosis of a high-voltage transmission line employing harmony search algorithm", *IET Generation, Transmission and Distribution*, vol. 4, no. 7, pp. 801–809, 2010.

[14] A. Askarzadeh, and A. Rezazadeh, "An innovative global harmony search algorithm for parameter identification of a PEM fuel cell model", *IEEE Transactions on Industrial Electronics*, vol. 59, no. 9, pp. 3473-3480, September 2012.

[15] K. Nekooei, Malihe M. Farsangi, Hossein N. and Kwang Y. Lee, "An improved multi-objective harmony search for optimal placement of DGs in distribution systems", *IEEE Transactions on Smart Grid*, vol. 4, no. 1, pp. 557-567, March 2013.

[16] Wasynczuk, O., D. T. Man, and J. P. Sullivan. "Dynamic Behavior of a Class of Wind Turbine Generators During Random Wind Fluctuations." *IEEE Trans. on Power Apparatus and Systems*, Vol. PAS-100, No, 6, pp. 2837-2845, 1981.

[17] S.M. Muyeen, M.H. Ali, R. Takahashi, T. Murata, Y. Tomaki, A. Sakahara and E. Sasano, "Comparative study on transient stability analysis of wind turbine generator system using different drive train models," *IET Renew. Power Gener.*, vol. 2, no. 2, pp. 131-141, 2007.

[18] L. Lopes and R. Almeida, "Wind-driven self-excited induction generator with voltage and frequency regulated by a reduced-rating voltage source inverter," *IEEE Trans. Energy Conv.*, vol. 21, no. 2, Jun 2006.

[19] G. Vachtsevanos and K. Kalaitzakis, A Hybrid Photovoltaic Simulator for Utility Interactive Studies, IEEE Trans. Energy Conversion, Vol. EC-2, No. 2, (June 1987), 227-231.

[20] Hany M. Hasanien, Ahmed S. Abd-Rabou, and Sohier. M. Sakr, "Design optimization of transverse flux linear motor for weight reduction and performance improvement using response surface methodology and genetic algorithms," *IEEE Transactions on Energy Conversion*, vol. 25, no. 3, pp. 598-605, September 2010.

[21] PSCAD/EMTDC Manual, Manitoba HVDC Research Center, 1994.

[22] Minitab, Minitab Inc. 2010, US.

[23] Release 2010 b, "MATLAB," The Math Works press, August 2010.